Available online at www.sciencedirect.com
ScienceDirect
Carbohydrate Research 343 (2008) 81–89
Carbohydrate RESEARCH

Macromolecular properties of cepacian in water and in dimethylsulfoxide

Yury Herasimenka,[a,†] Paola Cescutti,[a] Carlos E. Sampaio Noguera,[b] Josè R. Ruggiero,[b] Ranieri Urbani,[a] Giuseppe Impallomeni,[c] Flavio Zanetti,[d] Stéphane Campidelli,[e,‡] Maurizio Prato[e] and Roberto Rizzo[a,*]

[a]*Department of Biochemistry, Biophysics and Macromolecules Chemistry, University of Trieste, Via Licio Giorgieri 1, 34127 Trieste, Italy*
[b]*UNESP Sao Paulo State University, Department of Physics, IBILCE, Sao Jose do Rio Preto, Brazil*
[c]*Institute of Chemistry and Technology of Polymers, CNR, Viale A. Doria 6, 95125 Catania, Italy*
[d]*Eurand S.p.A., Area Science Park, Padriciano 99, 34012 Trieste, Italy*
[e]*Department of Pharmaceutical Sciences, University of Trieste, Piazzale Europa 1, 34127 Trieste, Italy*

Received 14 August 2007; received in revised form 5 October 2007; accepted 9 October 2007
Available online 13 October 2007

This paper is dedicated to the memory of Prof. Vittorio Crescenzi who introduced R. Rizzo to the fascinating world of polysaccharides

Abstract—Cepacian is the exopolysaccharide produced by the majority of the so far investigated clinical strains of the *Burkholderia cepacia* complex. This is a group of nine closely related bacterial species that might cause serious lung infections in cystic fibrosis patients, in some cases leading to death. In this paper the aggregation ability and the conformational properties of cepacian chain were investigated to understand its role in biofilm formation. Viscosity and atomic force microscopy studies in water and in mixed (dimethylsulfoxide/water) solvent indicated the formation of double stranded molecular structures in aqueous solutions. Inter-residue short distances along cepacian chain were investigated by NOE NMR, which showed that two side chains of cepacian were not conformationally free due to strong interactions with the polymer backbone. These interactions were attributed to hydrogen bonding and contributed to structure rigidity.

Keywords: Exopolysaccharide; *Burkholderia cepacia* complex; Biofilm; Conformational properties; Dimethylsulfoxide solutions

1. Introduction

The *Burkholderia cepacia* complex (Bcc) is a group of closely related bacteria that includes at least nine different species.[1] Some strains of the Bcc have been recognised as opportunistic pathogens for cystic fibrosis (CF) patients.[2] CF is an autosomal recessive disorder caused by mutations of the gene coding for the chloride ion-channel protein located in cell membranes of exocrine gland and secretory epithelial.[3] The consequence of the disease is the production of a viscous mucus on the surface of epithelia, including lungs.[4] Besides exocrine glands insufficiency, in lungs this thick fluid impedes the mucociliary clearance and favours the set-up of serious chronic infections by opportunistic pathogens that are very difficult to eradicate. Chronic airways infections and the accompanying inflammatory response cause heavy lung damages,

Abbreviations: AFM, atomic force microscopy; AMP, antimicrobial peptides; Bcc, *Burkholderia cepacia* complex; CF, cystic fibrosis; DMSO, dimethylsulfoxide; EPS, exopolysaccharide; M_n, number-average molecular mass; M_w, weight-average molecular masses

* Corresponding author. Tel.: +39 040 5583695; fax: +39 040 5583691; e-mail: rizzor@units.it
† Present address: FB Biologie/Chemie, Universität Osnabrück, Barbarastr. 11, 49076 Osnabrück, Germany.
‡ Present address: Laboratoire d'Electronique Moléculaire, CEA Saclay, 91191 Gif-sur-Yvette, France.

0008-6215/$ - see front matter © 2007 Elsevier Ltd. All rights reserved.
doi:10.1016/j.carres.2007.10.003

which are the major cause of premature death in CF patients.[4]

Studies carried out on *Pseudomonas aeruginosa*, one of the principal bacteria involved in CF lung infections, revealed that infection was associated with a switch from non-mucoid to mucoid phenotype characterised by overproduction of exopolysaccharide (EPS).[5] These biopolymers have been recognised as important virulence factors involved in a number of different mechanisms aimed at escaping the host defence machinery. As a matter of fact, EPS constitute the skeleton of biofilms that bacteria build around their colonies.[6] Biofilms act as suitable incubators for micro-organisms and, at the same time, form a physical barrier towards chemical agents potentially dangerous for bacteria's life. In addition, other relevant biological activities were recently recognised as specifically associated with EPS throughout their interaction with components of the immunological system. Herasimenka et al.[7] investigated the interaction between different bacterial EPS and antimicrobial peptides (AMP) of the innate immune system showing that the formation of molecular complexes caused the inhibition of antimicrobial activity, which impeded the lysis of the bacterial membrane by AMP. Woods and co-workers[8] found that bacterial capsular polysaccharides interacted with the C3b component of the host complement system thus impeding the binding of C3b on the bacterial surface and blocking the cascade of events that eventually led to bacteria's death. Finally, Bylund et al.[9] recognised that EPS inhibited neutrophyls chemiotaxis and scavenged the action of reactive oxygen species, thus lowering the efficiency of the host cellular response.

In our laboratory, the primary structure of EPS produced by several environmental and clinical strains of the Bcc has been investigated in detail.[10–14] It was found that different species of *Burkholderia* isolated from expectorates of CF patients produced at least five different EPS[13,15,16] although the one named cepacian (see Scheme 1 for the cepacian repeating unit) was synthesised by the majority of the strains investigated. This finding, together with those from different laboratories,[17,18] suggested us to consider cepacian as the EPS characteristic of the Bcc.

Previous investigation of the macromolecular and conformational properties of protonated cepacian chain in water proposed a rather rigid and extended conformation of the polysaccharide backbone with association of even number of chains in a multistranded structure.[19] An explanation of the chain rigidity in terms of intrachain hydrogen bonding was later given by molecular modelling studies.[20] Because these characteristics are relevant to understanding the role of cepacian in biofilm formation and its interaction with other biomacromolecules, the study of the macromolecular properties of cepacian was further pursued resorting to viscosity and atomic force microscopy both in water and in dimethylsulfoxide (DMSO), a solvent known to induce disruption of polymer chain aggregation in polysaccharides.[21] In addition, an NOE NMR investigation in water was carried out to determine the structural motifs responsible for chain rigidity.

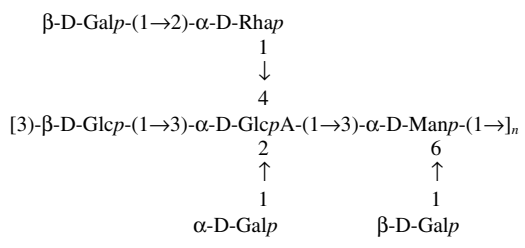

Scheme 1.

2. Experimental

2.1. Sample preparation

Cepacian was obtained from a clinical strain of *Burkholderia pyrrocinia* isolated at the Friuli Venezia Giulia Cystic Fibrosis Reference Center ('Burlo Garofolo Hospital', Trieste, Italy). *B. pyrrocinia* was grown as described.[13] The EPS was purified by isopropanol precipitation after removal of bacterial cells by centrifugation. After dialysis, the presence of protein and/or nucleic acid contaminants was checked by UV spectroscopy (260–280 nm). If necessary, the contaminants were eliminated by DNase, RNase and protease treatment. The polymer was always used as the Na^+ form. Cepacian de-O-acetylation was performed in 10 mM NaOH solution under nitrogen flux for 5 h at room temperature with magnetic stirring followed by dialysis and neutralisation.

2.2. Intrinsic viscosity

Intrinsic viscosity measurements were carried out with a Schott-Geräte AVS/G automatic viscometer using a Cannon-Ubbelohde capillary either with 0.53 mm internal diameter (high water-to-DMSO ratio) or 0.63 mm internal diameter (low water-to-DMSO ratio) thermostatted at 20 °C. The polymer solution was always added with a suitable amount of NaCl to a final concentration of 0.005 M to avoid polyelectrolytic effects during polymer dilution. Before measurements, solutions at high water-to-DMSO ratio were filtered on a 0.45 μm Millipore membrane, while those at low water-to-DMSO ratio were filtered on a 3 μm Millipore membrane.

2.3. Molecular weight measurement

Molecular weight measurements were carried out by HPSEC coupled with both light scattering (MALS

DAWN EOS, multiple angle light scattering, Wyatt Technology Co., USA) and refractive index (Optilab rEX, Wyatt Technology Co., USA) detectors. The data were processed by means of the ASTRA software, Ver. 5.1.9 (Wyatt Technology Co., USA). Three columns in series (TSK PW × 1 G6000, G5000 and G3000, 7.8 mm ID × 300 mm length, Tosoh Bioscience) were used for the chromatographic separation in water. For aqueous solutions measurements, a 0.05 M NaCl and 0.01% NaN_3 solution was used to dissolve the polymer. Before injection, the sample solution was filtered on a 0.45 μm Millipore membrane. The columns were thermostatted at 40 °C and a value of 0.141 mL/g was used as the specific refractive-index increment. For DMSO measurements, another column set (TSK gel Super AWM, 2 column in series plus a guard column AW-H, 4.6 mm ID × 150 mm length) was used. The sample solution was filtered on a 0.45 μm Millipore membrane, the columns were thermostatted at 40 °C and a value of 0.085 mL/g was used for the specific refractive-index increment. Both refractive index increments were measured on line by ASTRA software.

2.4. Atomic force microscopy

Atomic force microscopy experiments on cepacian aqueous solutions were performed spray-drying on a freshly cleaved mica surface a filtered polymer solution whose concentration was either 5 μg/mL or 30 μg/mL. For experiments carried out in 10% water/DMSO, a drop of polymer solution (either 5 μg/mL or 30 μg/mL) was allowed to dry onto a freshly cleaved mica surface for 3 days. The AFM apparatus was a Multimode Scanning Probe (Veeco) coupled with a control device Nanoscope IIIa. The tips, purchased from Veeco, were made of phosphorus-doped silicon.

2.5. NMR spectroscopy

NMR 2D-NOESY spectra were recorded in D_2O at 50 °C on a Varian ^{UNITY}INOVA instrument operating at 500 MHz using the standard Varian pulse sequence and a mixing time of 0.1 s. ^{1}H-chemical shifts were referenced to internal acetone (2.225 ppm).

3. Results and discussion

The structure of the repeating unit of cepacian (Scheme 1) is characterised by a backbone with (1→3) glycosidic bonds, three short lateral chains and a rather high degree of acetyl substitution (1–3 groups per repeating unit, depending on bacterial strains) as determined by NMR. Similar to other (1→3) linked carbohydrate polymers, for example, schizophyllan and scleroglucan, previous studies on cepacian[19] described the formation of chain aggregates with definite stoichiometry. To further determined the aggregation characteristics, the viscosity of cepacian was investigated in water and water–DMSO solutions where chains dissociation might occur, as reported for schizophyllan and scleroglucan.[22] The viscosity behaviour of native cepacian at different water-to-DMSO ratios is shown in Figure 1, where intrinsic viscosity data are reported for both native and de-O-acetylated samples. Due to the presence of uronic acid residues in the polymer repeating unit, the intrinsic viscosity was always measured in the presence of 5×10^{-3} M NaCl to lower intramolecular electrostatic repulsions. Under these conditions, the lowest solvent ratio used was 10% water in DMSO. On increasing the DMSO content, the intrinsic viscosity of both native and de-O-acetylated polymer solutions lowered; the value of the intrinsic viscosity in 10% water–DMSO was almost half that obtained in 100% water. The de-O-acetylated sample showed viscosity behaviour very similar to that of the native one, but characterised by slightly higher viscosity values throughout the range examined. As a matter of fact, in 60% water–DMSO solution the viscosity of the native (acetylated) polymer already decreased of about 7%, while the de-O-acetylated one still retained the same value exhibited in 100% water.

The decrease in solution viscosity observed at low water-to-DMSO ratios has two explanations: either it is a result of dramatic solvent-induced conformational transition or it is due to dissociation of a multistranded structure. To discriminate between these two possibilities, the molecular mass of the polymer in water and in DMSO was evaluated by use of high performance size exclusion chromatography coupled to a multi angle laser light scattering detector. The measurements were carried out on both native and de-O-acetylated samples and the data are reported in Table 1. The molecular mass values

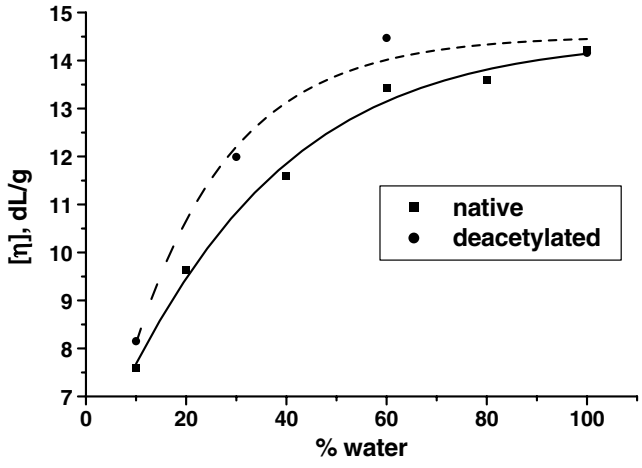

Figure 1. Intrinsic viscosity of native (■) and de-O-acetylated (●) cepacian in water–DMSO solutions as a function of water percentage.

Table 1. Molecular masses of native and de-O-acetylated cepacian in water and in DMSO

Polymer and solvent	M_w (kDa)	M_n (kDa)	M_w/M_n
Native cepacian in water	1660 ± 50	1280 ± 60	1.3
De-O-acetylated cepacian in water	1520 ± 30	1160 ± 60	1.3
Native cepacian in DMSO	1082 ± 30	650 ± 65	1.7
De-O-acetylated cepacian in DMSO	1015 ± 30	602 ± 70	1.7

correlated well with the viscosity data and indicated that cepacian forms aggregates in water. In addition, the molecular species present in water were dimeric with respect to those present in DMSO. Native and de-O-acetylated polymer forms identical types of aggregates in water and in DMSO; the de-O-acetylated sample exhibited a molecular mass slightly lower than that of native polymer due to the removal of acetyl groups. The similarity of the molecular masses also confirmed that the deacetylation reaction did not cause any significant degradation of the polymer. The number-average molecular mass (M_n) in DMSO was almost exactly half of that determined in water. However, the weight-average molecular masses (M_w) obtained in water solution did not show twice the value of those measured in DMSO, due to the larger contribution of high molecular weight fractions in the evaluation of M_w. It is worth noting that the polydispersity index (M_w/M_n, see Table 1), increased in passing from water to DMSO; this is expected as water contains associated species whereas DMSO contains largely dissociated species. When dissociated in DMSO, the polymers consist of a broad dispersion of small to large chains. However, the random association of the mixture of the small to large polymer chains are less likely to be comprised of chains of similar molecular mass thus resulting in a population of dimers characterised by a narrower polydispersity.

Further details of the association ability of cepacian chains were obtained by means of atomic force microscopy (AFM). AFM experiments on native and de-O-acetylated cepacian were carried out using samples from both aqueous and DMSO solutions. Two microimages obtained for the native polymer in water at different concentration are shown in Figure 2. The image at low concentration (5 μg/mL, Fig. 2a) shows individual molecular species of native cepacian characterised by an elongated polymer conformation with occasional ramifications. A few bent molecules were also detected. The image obtained at high concentration (30 μg/mL, Fig. 2b) shows the formation of a network due to multiple contacts between polymer chains. The statistical analysis of the thickness of the polymeric species, measured normal to the surface of the mica substrate, pointed at a large number of thick chain segments and a few thin segments. The average lateral dimension evaluated on the totality of the chains considered was 10.2 ± 1.5 Å. A typical vertical thickness measurement is shown in Figure 3.

A microimage of cepacian chains obtained starting from a 5 μg/mL concentration in 10% water–DMSO is shown in Figure 4. In general, the definition of these images was lower than those obtained from water solutions. Nevertheless, the network of polymer chains is well discernible and the average thickness of the objects can be measured by statistical analysis. Contrary to the images obtained for low concentration cepacian in water, no isolated molecules were detected from DMSO solutions. This observation might be explained taking into account a slow evaporation of DMSO from the mica surface with respect to pure water, and a different

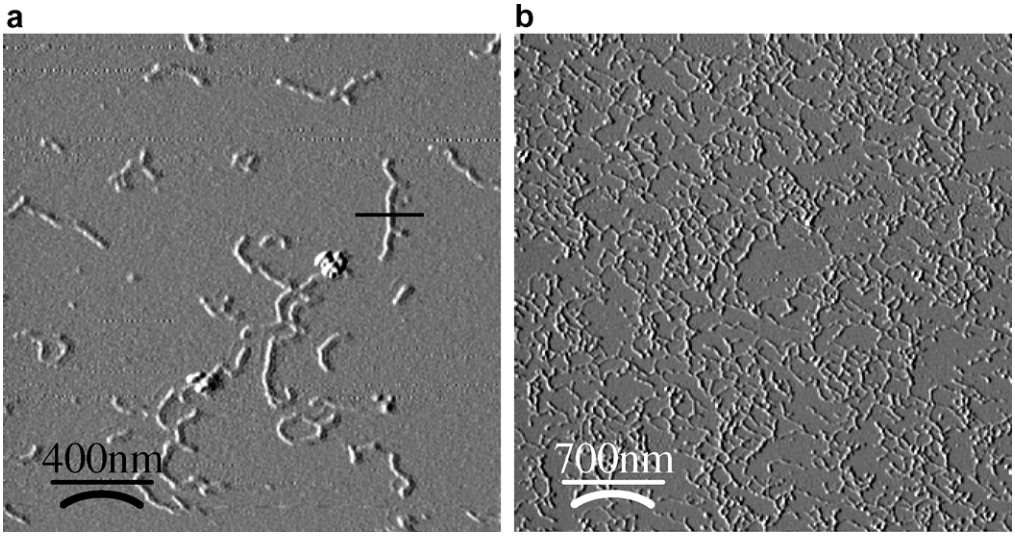

Figure 2. AFM images of native cepacian recorded in non-contact mode after spray-drying onto mica surface. (a, left) Polymer concentration 5 μg/mL in water. (b, right) Polymer concentration 30 μg/mL in water.

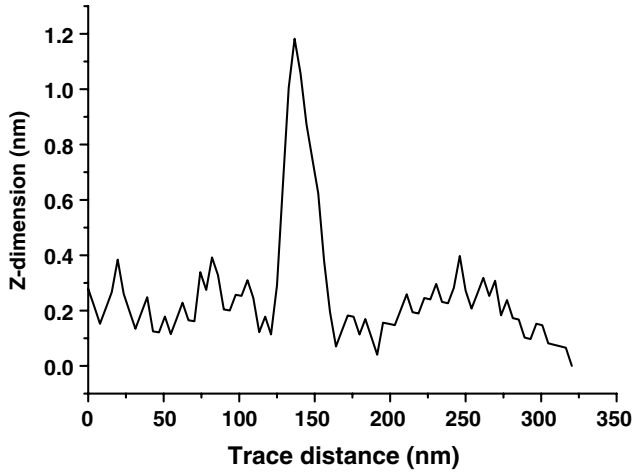

Figure 3. Trace through one polymeric species showing vertical height (taken from the vertical polymer image in Fig. 2, left, as shown by the black bar).

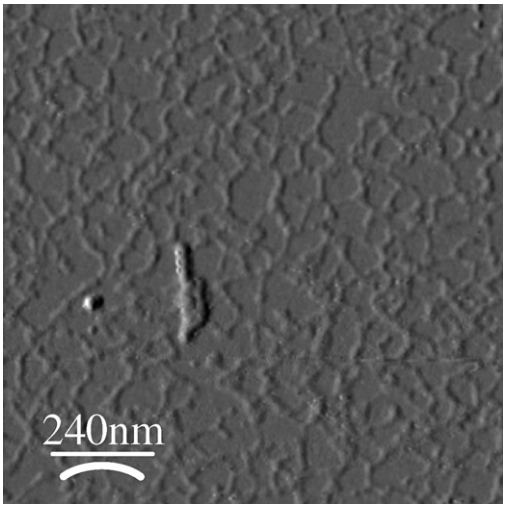

Figure 4. AFM image of native cepacian recorder in non-contact mode after evaporation on mica of a drop of a 10% water/DMSO solution. Polymer concentration 5 μg/mL.

polymer interaction with the mica surface in DMSO. These two factors probably resulted in the migration of EPS molecules towards the central part of the evaporating droplets, thus giving rise to a local increase of the solute concentration. The average polymer chain thickness obtained in DMSO was 6.1 ± 1.5 Å.

The cross-section value obtained in DMSO was almost half of that measured in water demonstrating that DMSO dissociated cepacian molecules and confirming that the chain complex in water was the dimeric form of the species present in DMSO. These AFM data are in very good agreement with both viscosity and molecular mass findings, additionally pointing at a mixture of polymeric species composed of double stranded structures, with occasional single stranded stretches. McIntire and Brant[23] obtained the value of 11.4 ± 3.0 Å for the thickness of the triple stranded structure of scleroglucan, a polysaccharide exhibiting, like cepacian, a backbone composed of (1→3) glycosidic bonds. This value is only slightly greater than that recorded for cepacian and can be explained by the lower number of side chains in scleroglucan (1) with respect to cepacian (3). In addition, the authors commented the discrepancy of the AFM value (11.4 Å) with respect to the value of 17.3 Å found for the triple stranded scleroglucan by X-ray fibre diffraction as probably due either to the distortion of polymer chains during dessication or to their interactions with the mica substrate. Taking into account the figures for scleroglucan, it is reasonable to conclude that the 10.2 Å value found for cepacian chains can be safely associated with the formation of double stranded structures.

Considering for cepacian the possible formation, within the polymer chains, of single and double stranded stretches with a thickness of 6 Å and 10 Å, respectively, the relative population of these two conformations in water is obtainable from AFM data. Taking the 8 Å value as the limit between single and double stranded structures, it turned out that the percentage of single stranded segments in water was 15% of the total. The average lateral dimension evaluated only on the chain population with a thickness higher than 8 Å was 10.6 ± 1.7 Å, which can be considered a more precise figure for the thickness of the double stranded structure.

AFM images were also acquired for de-O-acetylated cepacian. Images obtained for 5 μg/mL and 30 μg/mL polymer solutions in water are shown in Figure 5a and b, respectively. The statistical analysis of the thickness of the polymeric species revealed a percentage of single stranded chains segments (35%) higher than in the native polymer (15%). The average chain thickness, evaluated on the population of species with a cross-section larger than 8 Å, was 9.3 ± 2.0 Å, slightly lower than that obtained for the native polymer. This reduction in dimension might be explained with the formation of additional hydrogen bonds between the polymer main chain and the lateral chains due to an increased number of free hydroxyl groups after deacetylation. The more extended hydrogen bonding might also explain the slightly greater resistance of the double stranded de-O-acetylated structure to de-associate upon DMSO addition with respect to the native one, as shown by viscosity experiments. In addition, the higher percentage of single stranded chain stretches obtained upon deacetylation might indicate an important role of acetyl substituents in the biofilm formation.

The characteristic of cepacian to form double stranded structures is an important feature to understand the formation of cepacian biofilms because random dimerisation of polymer chains can explain the formation of the supramolecular network, which

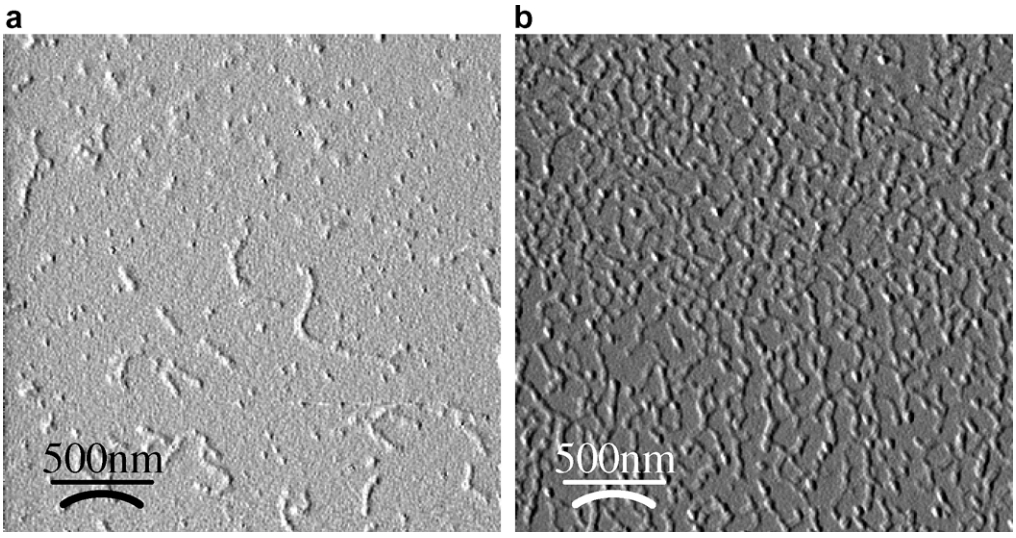

Figure 5. AFM images of de-O-acetylated cepacian recorded in non-contact mode after spray-drying onto mica surface. (left) Polymer concentration 5 μg/mL in water. (right) Polymer concentration 30 μg/mL in water.

constitutes the biofilm skeleton. Moreover, the intrinsic polymer chain rigidity is a further contribution to the physico-chemical properties of the biofilm. In a previous paper,[20] the conformational rigidity of cepacian backbone throughout the formation of intrachain hydrogen bonds was investigated by molecular modelling calculations. In the present paper the characterisation of the conformational rigidity of cepacian was further determined by means of 2D-NOE experiments. Because the position of acetyl groups on the cepacian backbone is not known yet, and to compare the NOE information with molecular modelling data, the NOE spectra were recorded on the de-O-acetylated sample. The NMR chemical shift assignments of de-O-acetylated cepacian are those reported.[10]

2D NOESY spectra were obtained on de-O-acetylated cepacian at 500 MHz and one section of the spectrum is reported in Figure 6. The spectrum contains a large number of cross-peaks. However, due to polymer chain dimerisation, cross-peaks may indicate both intramolecular and intermolecular short distances. Lacking a suitable model of chain association, only intramolecular NOE signals were considered. After cross-peak's assignment, the corresponding H–H interatomic distances were measured on the minimised structure of the three repeating unit fragment (21 sugar residues) as obtained by means of molecular modelling calculations (unpublished results), assuming the complete ionisation of uronic acids. NOE cross-peaks related to intramolecular distances higher than 5 Å were disregarded as they derived very likely from short intermolecular contacts. The analysis led to the selection of 12 NOE cross-peaks of interest not attributed to the trivial intra-residue contacts. The relevant data are reported in Table 2 and showed in Figure 6. The scheme of the NOE contacts on the cepacian repeating unit is reported in Figure 7.

The majority of NOE contacts indicated interactions either between lateral chains and main chain or within lateral chains. Other two contacts (marked as 6 and 7 in Table 2) involved two sugar residues of the main chain. The large number of NOE contacts involving the protons of the β-D-Gal*p*-α-D-Rha*p* dimeric side chain strongly indicated a low mobility of these sugar residues. In addition, the three NOE contacts between this lateral chain and the proton in position 4 of the glucuronic acid suggested a strong interaction between the lateral chain and the main chain. The two NOE contacts within the backbone further explained the chain stiffness exhibited by this polymer.

4. Conclusions

Bacterial polysaccharides contribute in different ways to create a micro-environment suitable for bacterial life. Besides interaction of EPS with molecular species potentially dangerous for bacteria, like components of the host immune system, the protective function of EPS is often provided by the formation of a biofilm around bacterial colonies, as it happens for strains of the *B. cepacia* complex and for *P. aeruginosa*. This structure is constituted of different components among which EPS play a critical role providing the structural matrix, which gives the suitable visco-elastic and porous properties required by bacteria. The characterisation of the macromolecular properties of cepacian obtained by means of viscosity and AFM experiments demonstrated that this EPS in water forms double stranded segments, which can be separated by the addition of DMSO as

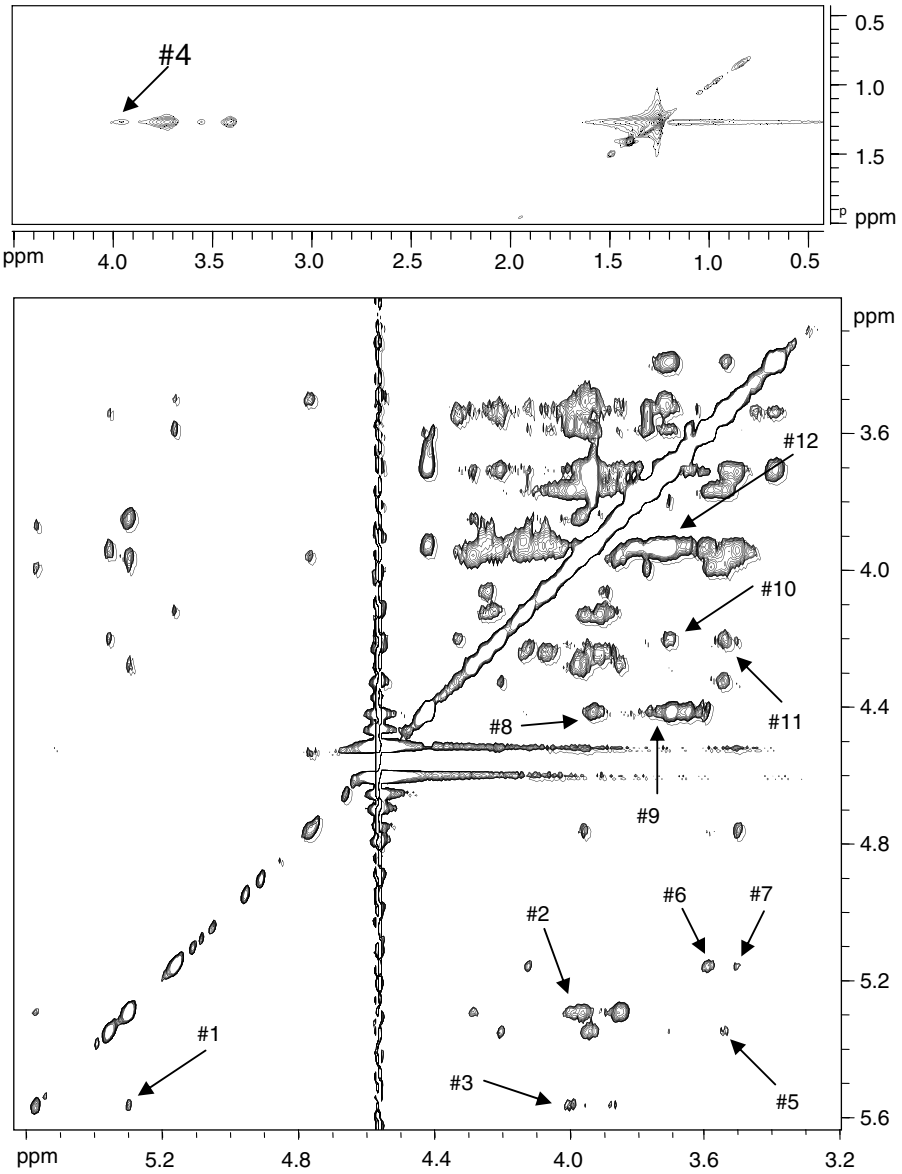

Figure 6. NOESY spectrum of de-O-acetylated and sonicated cepacian. Arrows indicate cross-peaks attributed to intramolecular H–H short distances. Upper: Rha*p* methyl resonances. Lower: ring proton resonances.

co-solvent. Ruling out the formation of perfect matches between two EPS chains, the interaction of a single polymeric molecule with two or more other molecules leads to the formation of a porous network, as revealed by AFM images obtained at relatively high polymer concentration. A schematic topological draw of the network is shown in Scheme 2.

The absence of acetyl groups notably decreased the percentage of double stranded stretches in the polymer structure so that it may be envisaged an important biological role for acetylation. This EPS modification might be used by bacteria to build a more compact biofilm and, consequently, the acetylation control might be a way to modulate the mechanical properties of biofilms.

Another contribution to the mechanical properties of biofilms is the intrinsic polymer chain rigidity. The presence of negatively charged groups on the cepacian backbone, commonly found in bacterial polysaccharides (e.g., alginate, which is produced by *P. aeruginosa*, is composed by uronic acids), certainly induces stiffness in the EPS chains due to repulsions between charges of the same sign. However, the presence of specific structural motifs can produce additional conformational rigidity by means of non-covalent intramolecular and intermolecular interactions, such as hydrogen bonding, so to further determine the mechanical properties of biofilms. In cepacian, this characteristic is given by the presence of strong interactions between the polymer backbone and lateral chains, as shown by NMR experiments.

Although biofilms are very complex systems where different biochemical processes, driven by bacterial cells

Table 2. NOE signals selected as intramolecular contacts

NOE contact #	Proton of residue 1	Proton of residue 2	ppm of the proton in residue 1	ppm of the D proton in residue 2	Interproton dist. from molecular modelling (Å)
1	α-D-Gal*p* (1)	α-D-GlcA*p* (1)	5.28	5.55	1.76
2	α-D-Gal*p* (1)	α-D-GlcA*p* (2)	5.35	4.02	2.60
3	α-D-Glc*p*A (1)	*t*-α-D-Gal*p* (3)	5.55	3.97	4.58
4	α-D-Glc*p*A (4)	α-D-Rha*p* (6)	3.96	1.27	4.63
5	α-D-Rha*p* (1)	*t*-β-D-Gal*p* (2)	5.37	3.56	4.49
6	α-D-Man*p* (1)	β-D-Glc*p* (3)	5.18	3.61	2.19
7	α-D-Man*p* (1)	β-D-Glc*p* (5)	5.17	3.53	4.07
8	*t*-β-D-Gal*p* (1)	α-D-Glc*p*A (4)	4.42	3.93	4.28
9	*t*-β-D-Gal*p* (1)	α-D-Rha*p* (3)	4.42	3.76	4.28
	t-β-D-Gal*p* (1)	α-D-Rha*p* (5)			4.38
10	α-D-Rha*p* (2)	*t*-β-D-Gal*p* (5)	4.21	3.70	4.20
11	α-D-Rha*p* (2)	*t*-β-D-Gal*p* (2)	4.20	3.54	4.49
12	α-D-Rha*p* (5)	α-D-Glc*p*A (4)	3.76	3.94	3.84

Numbers indicating the position of protons involved in short range contacts are indicated in parenthesis.

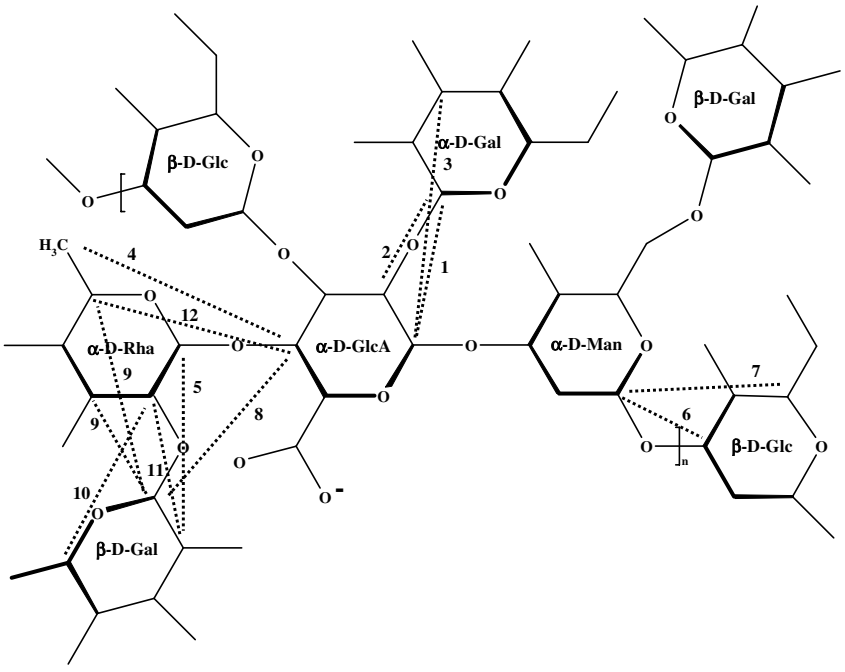

Figure 7. Schematic representation, on a segment of cepacian chain, of intramolecular H–H short distances as found by NOE investigation.

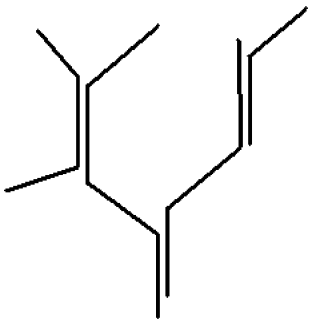

Scheme 2.

take place, the data obtained in this investigation gave a more detailed insight into the role played by polysaccharides in biofilm structure. Considering then the role of biofilm in bacterial infection, a more detailed knowledge of the three-dimensional architecture of the biofilm produced by *Burkholderia* spp. might suggest the design of suitable tools to disrupt the biofilm structure. These could be conveniently used in synergy with appropriate therapies for lung infections affecting cystic fibrosis patients.

Acknowledgements

This study was supported by a grant of the Friuli Venezia Giulia Regional Government (LR11/2003, Project No. 200502027001) and by the Italian Cystic Fibrosis

Foundation. The Kathleen Foreman Casali Foundation is gratefully acknowledged for a fellowship to Y.H.

References

1. Coenye, T.; Vandamme, P.; Govan, J. W. R.; LiPuma, J. J. *J. Clin. Microbiol.* **2001**, *39*, 3427–3436.
2. Mahenthiralingam, E.; Baldwin, A.; Vandamme, P. *J. Med. Microbiol.* **2002**, *51*, 533–538.
3. Kerem, B.-S.; Rommens, J. M.; Buchanan, J. A.; Markiewicz, D.; Cox, T. K.; Chakravarti, A.; Buchwald, M.; Tsui, L.-C. *Science* **1989**, *245*, 1073–1080.
4. Lyczak, J.; Cannon, C. L.; Pier, G. B. *Clin. Microbiol. Rev.* **2002**, *15*, 194–222.
5. Govan, J. W. R.; Deretic, V. *Microbiol. Rev.* **1996**, *60*, 539–574.
6. Branda, S. S.; Vik, Å.; Friedman, L.; Kolter, R. *Trends Microbiol.* **2005**, *13*, 20–26.
7. Herasimenka, Y.; Benincasa, M.; Mattiuzzo, M.; Cescutti, P.; Gennaro, R.; Rizzo, R. *Peptides* **2005**, *26*, 1127–1132.
8. Reckseidler-Zenteno, S. L.; De Vinney, R.; Woods, D. E. *Infect. Immun.* **2005**, *73*, 1106–1115.
9. Bylund, J.; Burgess, L. A.; Cescutti, P.; Ernst, R. K.; Speert, D. P. *J. Biol. Chem.* **2006**, *281*, 2526–2532.
10. Cescutti, P.; Bosco, M.; Picotti, F.; Impallomeni, G.; Leitão, J. H.; Richau, J.; Sá-Correia, I. *Biochem. Biophys. Res. Commun.* **2000**, *273*, 1088–1094.
11. Lagatolla, C.; Skerlavaj, S.; Dolzani, L.; Tonin, E. A.; Monti Bragadin, C.; Bosco, M.; Rizzo, R.; Giglio, L.; Cescutti, P. *FEMS Microbiol. Lett.* **2002**, *209*, 99–106.
12. Cescutti, P.; Impallomeni, G.; Garozzo, D.; Sturiale, L.; Herasimenka, Y.; Lagatolla, C.; Rizzo, R. *Carbohydr. Res.* **2003**, *338*, 2687–2695.
13. Chiarini, L.; Cescutti, P.; Drigo, L.; Impallomeni, G.; Herasimenka, Y.; Bevivino, A.; Dalmastri, C.; Tabacchioni, S.; Manno, G.; Zanetti, F.; Rizzo, R. *J. Cystic Fibr.* **2004**, *3*, 165–172.
14. Herasimenka, Y.; Cescutti, P.; Impallomeni, G.; Campana, S.; Taccetti, G.; Ravenni, N.; Zanetti, F.; Rizzo, R. *J. Cystic Fibr.* **2007**, *6*, 145–152.
15. Cèrantola, S.; Marty, N.; Montrozier, H. *Carbohydr. Res.* **1996**, *285*, 59–67.
16. Conway, B. A.; Chu, K. K.; Bylund, J.; Altman, E.; Speert, D. P. *J. Infect. Dis.* **2004**, *190*, 957–966.
17. Cérantola, S.; Lemassu-Jacquier, A.; Montrozier, H. *Eur. J. Biochem.* **1999**, *260*, 373–383.
18. Linker, A.; Evans, L. R.; Impallomeni, G. *Carbohydr. Res.* **2001**, *335*, 45–54.
19. Sist, P.; Cescutti, P.; Skerlavaj, S.; Urbani, R.; Leitão, J. H.; Sá-Correia, I.; Rizzo, R. *Carbohydr. Res.* **2003**, *338*, 1861–1867.
20. Sampaio Noguera, E. C.; Ruggiero, J. R.; Sist, P.; Cescutti, P.; Urbani, R.; Rizzo, R. *Carbohydr. Res.* **2005**, *340*, 1025–1037.
21. Sato, T.; Norisuye, T.; Fujita, H. *Carbohydr. Res.* **1981**, *95*, 195–204.
22. Yanaki, T.; Norisuye, T. *Polym. J.* **1983**, *15*, 389–396.
23. McIntire, T. M.; Brant, D. A. *Biopolymers* **1997**, *42*, 133–146.